**Climate
of the Past
Discussions**

# Glacial-interglacial vegetation dynamics in south eastern Africa depend on sea surface temperature variations in the west Indian Ocean

L. M. Dupont[1], T. Caley[2], J.-H. Kim[3], I. Castaneda[3], B. Malaizé[2], and
J. Giraudeau[2]

[1]MARUM Center for Marine Environmental Sciences, University of Bremen, Bremen, Germany
[2]Université de Bordeaux 1, UMR5805, EPOC, CNRS – Bordeaux, France
[3]NIOZ Royal Netherlands Institute for Sea Research, Department of Marine Organic
Biogeochemistry, Texel, The Netherlands

Discussion Paper | Discussion Paper | Discussion Paper | Discussion Paper |

CPD

7, 2261–2296, 2011

**Glacial-interglacial
vegetation dynamics
in south eastern
Africa**

L. M. Dupont et al.

Title Page

Abstract | Introduction

Conclusions | References

Tables | Figures

◄ | ►|

◄ | ►

Back | Close

Full Screen / Esc

Printer-friendly Version

Interactive Discussion

## Abstract

Glacial-interglacial fluctuations in the vegetation of South Africa might elucidate the climate system at the edge of the tropics between Indian and Atlantic Ocean. However, vegetation records covering a full glacial cycle have only been published from the east-
5  ern South Atlantic. We present a pollen record of the marine core MD96-2048 retrieved by the Marion Dufresne from the Indian Ocean ~120 km south of the Limpopo River mouth. The sedimentation at the site is slow and continuous. The upper 6 m (down till 342 ka) have been analysed for pollen and spores at millennial resolution. The terrestrial pollen assemblages indicate that during interglacials the vegetation of eastern
10 South Africa and southern Mozambique largely consisted of evergreen and deciduous forests. During glacials open mountainous scrubland dominated. Montane forest with *Podocarpus* extended during humid periods favoured by strong local insolation. Correlation with the sea surface temperature record of the same core indicates that the extension of mountainous scrubland primarily depends on sea surface temperatures
15 of the Agulhas Current. Our record corroborates terrestrial evidence of the extension of open mountainous scrubland (including elements with affinity to the Cape Flora) for the last glacial as well as for other glacial periods of the past 300 ka.

## 1  Introduction

South Africa sits at the edge of the tropics between the Indian and Atlantic Oceans.
20 Today, only the tip of South Africa reaches into the sub-tropical winter rain area touched by the circum-Antarctic Westerlies at their northernmost winter position. The eastern part of South Africa presently has a tropical summer rain climate strongly depending on the sea surface temperatures (SSTs) of the Southwest Indian Ocean and the influence of the Agulhas Current (e.g. Jury et al., 1993; Tyson and Preston-Whyte, 2000).
25   There has been a long standing debate over how South African climate and vegetation changed through the Pleistocene glacial-interglacial cycles. Some authors

advocate a shift of the winter rainfall area northwards during glacial times but differ about the amplitude of that shift (e.g. Heine, 1982; Stuut et al., 2004; Shi et al., 2001; Chase, 2010). Others argue that most of South Africa, especially the southern Cape remained under summer rain influence (Lee-thorp and Beaumont, 1995; Partridge et al., 1999; Bar-Matthews et al., 2010). See for full discussion Chase and Meadows (2007) and Gasse et al. (2008) and references therein. Not only is the latitudinal position, intensity, and influence of the Westerlies, and with it the extent of the summer rainfall area insufficiently clarified, but the impact of local versus Northern Hemisphere insolation on the climate of South Africa is also largely unknown. The age model of the Tswaing Crater sequence (Partridge et al., 1997; Kirsten et al., 2007) is heavily tuned to precession and cannot be stated as independent evidence for the impact of local insolation. The debate is thus fuelled by the lack of good records to address the climate cycle of land-cover change in Southern Africa. Even for the last Glacial the terrestrial evidence is fragmentary, poorly dated or contradictory. Records integrating a full glacial-interglacial cycle or spanning more than one climate cycle are only covered by marine cores.

Yet, understanding fluctuations in vegetation and land-cover – which have shaped the environment of early humans (e.g. Marean et al., 2007; Wadley, 2007; Chase, 2010; Henn et al., 2011) – is critical as they are related to globally important systems such as the Agulhas and Benguela Currents, the latitude of the Subtropical Front, and the position of the sub-tropical high-pressure systems in the Southern Hemisphere. Furthermore, vegetation records can be used to validate results from earth system dynamic vegetation models of high or intermediate complexity.

In the present paper we focus on the regional development of the vegetation of south Mozambique and the northeast corner of South Africa since 350 ka BP. We study vegetation change and SST estimates (Caley et al., 2011) over several glacial-interglacial cycles to better understand the driving forces of land-cover variations in the region using sediments of a marine core retrieved nearby the mouth of the Limpopo River. The glacial-interglacial vegetation variability in the marine core is compared to the

Title Page

Abstract | Introduction

Conclusions | References

Tables | Figures

◄◄ | ►►

◄ | ►

Back | Close

Full Screen / Esc

Printer-friendly Version

Interactive Discussion

pollen records of Wonderkrater (Scott, 1982a; Scott et al. 2003) and Tswaing Crater (Scott, 1999, Scott and Tackerey, 1987) in South Africa and to the pollen record of Lake Tritrivakely on Madagascar (Gasse and Van Campo, 1998, 2001).

The study area to-day is well south of the influence of the tropical convergence zone. At this stage we do not attempt to compare with the records of Lake Malawi (DeBusk, 1998; Cohen et al., 2007; Beuning et al., 2011), Lake Masoko (Vincens et al., 2007), or Kashiru (Bonnefille and Riollet, 1988), which are situated too far north to be used as a guide for the region and are, therefore, beyond the scope of this paper. A more comprehensive review of vegetation changes in Africa over several climatic cycles is in preparation.

## 2   Topography and modern climate

Extensive lowlands stretch north of the site intersected by the floodplains of the Limpopo and the Changane Rivers (Fig. 1). The floodplain soils of the Changane River are salty (Kersberg, 1985, 1996). West of Maputo, the relief rises to the central plateau of southern Africa. The Great Escarpment forms here the northern part of the Drakensbergen (up to over 2000 m a.s.l.). Between the escarpment and the coast lies a N-S oriented low ridge, the Lebombos hills (100–500 m a.s.l.).

The average annual temperature ranges from 16 °C on the central plateau to 24 °C in the lowland area. Lowlands are devoid of frosts, but the highland can have severe frosts during clear winter nights (Kersberg, 1996). Average annual precipitation ranges from 1400 mm in the mountains to 600 mm in the lowlands. Rain falls mostly in summer (November to March). Because of the relief of the Great Escarpment temperature and rainfall contours are N-S directed. Along the coast rain is more frequent. The warm waters of the Agulhas Current system bring warm and humid air over the lowland into the mountains of the Escarpment. Rainfall during late summer in the region increases with warmer sea surface temperatures (SST) of the Agulhas Current. However, rainfall

diminishes when SST of the western Southwest Indian Ocean decrease (Jury et al., 1993; Reason and Mulenga, 1999).

The area lies in the transition between tropical and subtropical climate, just south of the subtropical ridge between the southern Hadley and the Ferrel cell (Tyson and Preston-Whyte 2000). Most of the year surface airflow is from east to west and stronger during summer. During winter the average wind direction turns southwest in June to northeast in September, but winds tend to be weak. The topographic configuration of the high interior, the escarpment and the coastal lowland creates coastal low pressure cells that travel eastwards from Cape Town along the coast and are associated with Bergwinds blowing down the mountains in offshore direction (Tyson and Preston-Whyte, 2000). On a daily basis, mountain winds blow offshore by night (land breeze) and onshore by day (sea breeze).

On days without rain, stable layers at about 500 hPa and 700 hPa develop over southern Africa. Between these stable layers dust and aerosols can be trapped, re-circulated over the continent for days and finally exported over large distances over the oceans, to the Atlantic but mainly to the Indian Ocean (>75 %) (Tyson and Preston-Whyte, 2000). However, the transport takes place above the marine boundary layer and is thus of little consequence for the pollen delivery to our marine site close to the coast.

## 3 Modern vegetation

The vegetation in the region is very varied (Fig. 1) and is classified into as much as five different phytogeographical regions (phytochoria after White, 1983). Two tropical phytochoria, the Zambezian interior and the Zanzibar-Inhambane coastal region; two tropical-subtropical ones, the Highveld and the coastal Tongaland-Pondoland region; and one belonging to the Afromontane region (White, 1983). The natural vegetation ranges from closed forest to dry scrubland and from alpine open grassland to semi-evergreen lowland forest. Along the rivers wet forest alternates with floodplain savannahs and herb communities. However, most of the floodplain is now under

cultivation. The saline soils along the Changane River carry halophytic plants such as *Arthrocneum* and *Atriplex* of the Chenopodiaceae family. Seasonally flooded flat depressions east of the Changane River bear a palm and termite savannah with *Hyphaene*, *Phoenix*, *Acacia*, *Garcinia*, *Cyperus*, *Phragmites* and other grasses (Kersberg, 1985, 1996).

Closed forest is found in the form of cloud forest (with a rich flora including *Podocarpus*) and semi-deciduous forest on the Drakensbergen, riparian forest and coastal forest in the lowland, and mangroves along river estuaries. North of the site, in the Zambezian region, Miombo woodland (with *Brachystegia*) and Mopane dry woodland (with *Colophospermum mopane*) occur. Several types of woodland and scrubland with ticket or grass stratum are found in the lowlands west and northwest of the city of Maputo and on the Lebombos hills. Thicket also covers the littoral dunes. Woody savannahs occur in the higher parts along the Great Escarpment and the elevated inland plateau, the Highveld, is covered by open grasslands (Kersberg, 1985, 1996).

Along the coast north of the marine site, the littoral dunes are closely covered by evergreen hemi-sclerophyllous thicket. Behind the narrow coastal strip closed forest in the form of evergreen seasonal to semi-deciduous lowland forest is found on the sub-littoral belt of ancient dunes. Behind the sub-littoral, Miombo woodland with *Brachystegia* grows northeast of the Limpopo River and comparable woodland, with *Sclerocarya* but without *Brachystegia* grows southwest of the river. Shrubland with *Combretum*, *Philenoptera*, *Ziziphus*, and *Acacia* exists between the Limpopo and Incomati Rivers. South and west of it, scrub savannah with *Acacia*, *Sclerocarya*, *Combretum*, *Ziziphus*, and *Peltophorum africanum* covers the lowland area west and east of the Lebombos hills (Kersberg, 1985, 1996).

## 4   Material and methods

The marine core MD96-2048 (26°10′ S 34°01′ E, Fig. 1) was retrieved by the Marion Dufresne cruise MOZAPHARE (MD 104) at 660 m water depth on the upper continental

Title Page

Abstract | Introduction

Conclusions | References

Tables | Figures

◄ | ►

◄ | ►

Back | Close

Full Screen / Esc

Printer-friendly Version

Interactive Discussion

slope east of Maputo and south of the mouth of the Limpopo River. The shelf here is rather broad and the continental slope is not very steep. The southern directed flow of warm waters of the Agulhas Current system is structured in counter clockwise eddies but for the shallower area along the coast (Lutjeharms and da Silva, 1988).
⁵ The clockwise current along the coast off Maputo forms an eddy, which flow slows in the centre where suspended material settles (Martin, 1981). Our site is located in the northern part of the southern Limpopo cone depot centre which is built up since Late Miocene times (Martin, 1981).

The material has been retrieved at 660 m water depth by giant piston coring. The age
¹⁰ model of MD96-2048 is constructed by correlating the stable oxygen isotopes of the benthic foraminifer *Planulina wuellerstorfi* to the global reference stack LR04 (Lisiecki and Raymo, 2005; Caley et al., 2011). The oxygen isotope stratigraphy indicates a rather slow, but continuous sedimentation rate. For this study 116 samples from the upper 6 m covering the past 342 ka (MIS 9 to 1) have been palynologically analysed by
¹⁵ the first author.

Samples of 3 to 7 ml were taken every two to five cm from the upper 6 m. Volume was measured using water displacement. Samples were decalcified with diluted HCl (∼12 %) and after washing treated with HF (∼40 %) for several days to remove sili-cates. Two *Lycopodium* spore tablets containing $10\,680 \pm 1.8$ % markers each were
²⁰ added during the decalcification step. Samples were sieved over a cloth with meshes of 8 μm (diagonal) using ultrasonic treatment, which resulted in the removal of particles smaller than 10–12 μm. If necessary the sample was decanted to remove remaining silt. Samples were stored in water, mounted in glycerol, and microscopically examined (magnification 400 and 1000x) for pollen, spores, and dinoflagellate cysts by the first
²⁵ author. Pollen (Table 1) was identified using Scott (1982b), the African Pollen Database http://medias3.mediasfrance.org/pollen/, and the reference collection of African pollen grains of the Department of Palynology and Climate Dynamics of the University of Göttingen.

Title Page

Abstract | Introduction

Conclusions | References

Tables | Figures

◀ | ▶|

◀ | ▶

Back | Close

Full Screen / Esc

Printer-friendly Version

Interactive Discussion

Two types of time-series analysis have been carried out, Wavelet analysis after Torrence and Compo (1998) and cross spectral analysis using AnalySeries 2.0 (Paillard et al., 1996). To create equidistant series for spectral analysis endmember abundances were re-sampled every 3 ka between 0 and 342 ka. The Wavelet analysis applied a Mortlet 6.00 wavelet, zero padding and a white-noise background spectrum http://paos.colorado.edu/research/wavelets/. Cross spectral analysis has been performed after the Blackman-Tuckey method using a Bartlett Window with 35 lags resulting in a bandwidth of 0.0142857. Errors and coherency have been calculated for the 95 % confidence level (non-zero coherency > 0.554094; error estimate 0.486146 < Δ Power/Power < 3.11201). To check the significance of the power maxima in the frequency domain we used the f-test of the Multi-Taper-Method.

## 5 Results

### 5.1 Pollen concentration and percentages of selected pollen taxa

Percentages are calculated based on the total number of pollen and spores and selected curves are plotted in Figs. 2 and 3. The material varied strongly in the amount of palynomorphs. Therefore, not all samples could be counted to a desirable pollen sum of 300 or more. Most sums vary between 100 and 390 pollen and spores, but in a few cases not even 100 pollen and spores could be found. The calculation sum is depicted in Fig. 2. Percentages are based on the total of pollen and spores. The pollen concentration per mL and a summary diagram are given in Fig. 3. The age model (after Caley et al., 2011) is constructed by comparison of the stable oxygen isotope curve of benthic foraminifers to the stack of LR04 (Lisiecki and Raymo, 2005).

Pollen concentration per ml is rather low, mostly less than 2000 grains per mL and lower in the older part of the studied sequence between 340 and 120 ka than in the younger part after 120 ka. Maxima of more than 4000 grains per mL are found at

depths dated around 115, 90, 70, and 60–40 ka. After 40 ka pollen concentrations are again low and decline further after 15 ka (Fig. 3).

215 pollen taxa have been identified, 108 taxa turned up in more than 5 samples (Table 1). Most abundant pollen is from *Podocarpus* (yellow wood), Cyperaceae
5 (e.g. sedges), and Poaceae (grasses). Pollen taxa have been grouped in pollen from (a) forest trees, (b) woodland trees and scrubs, (c) mountainous herbs, scrubs and trees, (d) coastal and halophytic scrubs and herbs, (e) riparian and swamp plants based on Kersberg (1996) and Coates Palmgrave (2002). Asteraceae (without *Stoebe*-type and *Tarchonanthus*/*Artemisia*-type), Cyperaceae, Poaceae, *Podocarpus*, and *Rhi*-
10 *zophora* (mangrove tree) pollen are not placed in one of the groups mentioned above. Percentages of selected pollen taxa and groups calculated on the basis of total of pollen and spores are given in Fig. 2.

Pollen of woodland scrubs and trees as well as forest trees show maximum percentages during marine isotope stages (MIS) 9, 7, 5, and 1. Three successively declining
15 percentage maxima are found for MIS 5. Fern spore percentages vary between 4 and 16 % with maxima during early MIS 7, early MIS 5, and MIS 1. Pollen of coastal and halophytic scrubs and herbs is not abundant. Most of this pollen is found parallel to the forest maxima. Also *Rhizophora* pollen is not abundant with maxima during early MIS 9 and early MIS 5. *Podocarpus* pollen percentages show maxima during termi-
20 nations and the cooler phases of MIS 7 and 5. Pollen of mountainous scrubs and trees, including Ericaceae (heather), has low percentages during most of MIS 9, 7, 5, and 1. Percentages for this group show maxima during MIS 8, 6, and 4–2. Poaceae pollen percentages run parallel to those of the mountainous group except for maxima in MIS 7, early MIS 5, and late MIS 1. Cyperaceae pollen is relatively abundant with
25 percentages between 10 and 40 %. Minima are found in MIS 9 and early MIS 5. Pollen of other riparian and swamp plants has a conspicuous maximum just before 100 ka.

Title Page

Abstract | Introduction

Conclusions | References

Tables | Figures

◀◀ | ▶▶

◀ | ▶

Back | Close

Full Screen / Esc

Printer-friendly Version

Interactive Discussion

## 5.2 Endmembers

We carried out a multivariate analysis in the form of an endmember model unmixing procedure (Weltje, 1997), which statistics are specifically designed for the treatment of percentage data using a version of the unmixer algorithm programmed in MATLAB by Dave Heslop in 2008. Taxa occurring in at least 5 different samples (listed in Table 1) are used in the endmember modelling (total of 108 taxa and 116 samples). We used a model with three components (EM1, EM2, EM3) explaining over 93 % of the variance ($r^2 = 0.935$). Iteration was stopped at 1000 resulting in a convexity at termination of 1.92. The scores of the pollen taxa on the endmembers are given in Table 1.

The endmembers "consist" of a mixture of pollen and spore taxa, whereby the focus within each endmember clearly differs (Figs. 4–6, Table 1). EM1 is dominated by the variability in the *Podocarpus* pollen abundance. Other significant contributions to EM1 are of Schizaceae (tree ferns), Alismataceae, *Celtis*, *Hymenocardia*, *Peltophorum africanum*, and *Myrsine africana*. In EM2 Cyperaceae pollen fluctuations are dominant and the variability of Ericaceae pollen and *Phaeoceros* (hornwort) spores is important together with that of Asteroideae and Poaceae pollen. Other significant contributions are of *Stoebe*-type, *Passerina*, Restionaceae (cape reeds), *Typha* (cattail), and *Lycopodium cernuum* (clubmoss). A large number of pollen taxa from forest and woodland (*Alchornea*, Combretaceae, *Khaya*-type, etc.) and mangroves (*Rhizophora*) score on EM3. Also important for EM3 are the relative abundances of Chenopdiaceae/Amarantaceae, Poaceae, *Cotula*-type and other Asteroideae, and *Anthospermum* pollen.

The relative abundances of the endmembers plotted against time (Fig. 3) show a strong pattern of interglacial-glacial fluctuations, whereby EM3 is most abundant during interglacials (MIS 9, 7, 5e, and 1) and EM2 most abundant during glacials (MIS 8, 6, and 4 to 2). Additionally EM3 reaches 0.4 during MIS 3 and short phases in MIS 6 and early MIS 8. EM1 scores during the intermediate periods.

# 6 Discussion

## 6.1 Source region of pollen and spores

Generally, the atmospheric circulation is not favourable for pollen transport to the marine site. Only Bergwinds and nightly land breezes (Tyson and Preston-Whyte, 2000) might carry pollen and spores directly from the Drakensbergen and lowlands west of Maputo. On average, weak north and northeast winds might deliver pollen and spores during the late winter season. On the other hand, the site is situated less than 120 km from the coast and the mouth of the Limpopo River, which catchment covers a large area including parts of northern South Africa, Zimbabwe, and Mozambique. Because of the relative short distance to the coast and the location of the site on the southern Limpopo cone depot centre (Martin, 1981), we expect most pollen and spores to be fluvial. Therefore, the source region is sought mainly north of Maputo from the Drakensbergen in the west to the coastal plain in the east. Results of organic geochemistry performed on the same sediments indicate that the relative amount of terrestrial soil material in the core is very low (Caley et al., 2011) and consequently low is the pollen concentration per mL sediment.

## 6.2 Glacial-interglacial vegetation changes

The three endmembers, EM1, EM2, and EM3 being distinguished by the unmixer algorithm can be interpreted as the representation of one or more vegetation complexes. EM1 (Fig. 4, Table 1) probably represents rather humid mountainous *Podocarpus* forest and combines *Podocarpus* values with values of woodland taxa such as *Peltophorum africanum* and *Celtis*, the Highveld taxon *Myrsine africana*, and taxa indicating moist conditions such as Alismataceae and tree ferns (Schizaceae). As *Podocarpus* values are the main constituent of EM1, *Podocarpus* pollen percentages and EM1 abundances show similar trends. However, it should be kept in mind, that *Podocarpus* is generally overrepresented by its pollen (Coetzee, 1967). Types of humid mountain

forests probably were wide-spread and might even have grown in the valleys during MIS 9, MIS 7, and the later part of MIS 5. In the course of MIS 8 *Podocarpus* forest became successively more important. During the Holocene the mountain forest probably was much reduced.

EM2 (Fig. 5, Table 1) mainly represents the open mountain vegetation dominated by ericaceous scrubs (Ericaceae and some Asteroideae) together with a strong swampy component indicated by high scores of Cyperaceae, *Stipularia africana*, and *Typha*. Other mountain elements such as *Passerina*, *Stoebe*-type, and Restionaceae indicate a link with Fynbos vegetation (nowadays growing at the Cape). Furthermore hornwort (*Phaeoceros*) and clubmoss (*Lycopodium*) occur. EM2 is most abundant during full glacials (MIS 8, 6, 2 to 4) indicating open mountainous habitats were common and spread to lower altitudes. Woody vegetation and forest probably was sparse. Rivers could have been fringed with open swamps dominated by sedges and some grasses instead of gallery forest.

EM3 combines pollen taxa from woodland and forest (Fig. 6, Table 1) with those of the coastal vegetation (*Tribulus*), mangroves (*Rhizophora*), and halophytes (Chenopodiaceae/Amaranthaceae) on saline soils. *Anthospermum* and Poaceae from the Highveld grasslands are also represented. In combining such a variety of taxa, EM3 probably records the complex of different biomes not unlike the modern situation mainly occurring during interglacial stages (MIS 9, 7, 5e, and 1).

Thus, three complexes of biomes can be distinguished for the region north and west of Maputo (northern South Africa and southern Mozambique). During most of the glacial periods mountainous scrubland was important, during relatively warm and humid parts of the glacial mountainous *Podocarpus* forest extended, and during interglacial periods the vegetation consisted of a complex of woodland and forest in the lowlands and grasslands on the interior plateau. This pattern has been consistent over the past three glacial-interglacial cycles.

Compared to the record of the marine site MD79-254 situated in front of the Zambezi River (Van Campo et al., 1990), the pollen percentage maximum of Ericaceae

Title Page

Abstract | Introduction

Conclusions | References

Tables | Figures

◄ | ►◄

◄ | ►

Back | Close

Full Screen / Esc

Printer-friendly Version

Interactive Discussion

is slightly higher (7.8 % at the Limpopo compared to 5.7 % at the Zambezi) and that of Combretaceae lower (2.7 % instead of 8.0 %, respectively). The higher Ericaceae and lower Combretaceae relative abundance at the southern site is consistent with a poleward decrease in temperatures.

## 6.3 Extent of the open mountain vegetation during glacials

Strong increase of mountain vegetation during glacials has also been found in other records of southern African vegetation (e.g. Scott, 1982a, 1999; Gasse and Van Campo, 2001). West of the marine site MD96-2048, at Tswaing Crater (Scott, 1999; Scott and Tackerey, 1987) pollen from various vegetation types were found such as *Podocarpus* from mesic forest, Combretaceae, *Burkea africana*, and *Spirostachys* from warm savannah woodland, and *Tarchonanthus* from the dry savannah of the Kalahari "thornveld". During the glacial parts of the sequence *Artemisia*, *Stoebe*-type, *Passerina* and Ericaceae from cool or temperate shrubland and Fynbos became important. Also in east South Africa, the sequence of Wonderkrater springs (Scott, 1982a) indicates a change from mostly cool upland vegetation types during the Glacial and the deglaciation to bushland during the Holocene, which is congruent with our results. According to the terrestrial evidence, the last Glacial vegetation included *Podocarpus* mesic forest and "bushveld" with Asteraceae, *Anthospermum*, *Cliffortia*, *Passerina*, Ericaceae, and *Stoebe* alternating with more open grassland communities. During the Holocene, a Kalahari type "bushveld" with Combretaceae, Capparaceae, *Burkea africana*, *Acacia*, *Peltophorum africanum* and denser woodlands with *Olea* and Proteaceae occurred (Scott, 1982a).

A comparable pattern of glacial-interglacial vegetation changes is found on Madagascar recorded at Lake Tritrivakely (Gasse and Van Campo, 1998, 2001), where the glacial vegetation dominated by Ericaceae changed to a mosaic of open canopy vegetation (Poaceae, Asteraceae, Chenopodiaceae) alternated with woodland (*Celtis*, Combretaceae, *Macaranga*-type, *Uapaca*) or mountainous forest with *Podocarpus*, *Dombeya*, and *Vitex*. Putting the evidence of several pollen sequences in South Africa

and Madagascar (Scott, 1987, 1989, 1999l; Botha et al., 1992; Scott and Woodborne, 2007, and opt cit.) together indicates that cool upland vegetation types, in the terminology of Scott (1999), might have dominated the south African sub-continent during glacial periods. It is comparable to the xerophytic woods and scrubs biome mapped by Elenga et al. (2000) being prominent in the Rift Valley during the Last Glacial Maximum.

The existence of cool upland vegetation over both eastern and southern South Africa during long periods of time might have provided favourable conditions (at least compared to some other parts of tropical Africa; e.g. Cohen et al., 2007) for early humans during the Middle Stone Age. Numerous Middle Stone Age sites located mostly along the south coast of South Africa (e.g. Jacobs et al., 2008; Henshillwood et al., 2001, 2009), but also along the eastern Escarpment (Wadley, 2007), have been found and dated indicating that modern behaviour in humans might have emerged in the region early, 75–100 ka ago or even earlier (Marean et al., 2007). Other lines of evidence indicate that the hunter-gatherer populations of southern Africa are genomically diverse and distinct from agriculturalists suggesting a southern African origin for modern humans (Henn et al., 2011).

## 6.4 Effects of SST of the Agulhas Current on the vegetation development

The pattern of vegetation change registered at MD96-2048, on the South African continent and on Madagascar suggests a strong impact of glacial climate. The extension of the mountain vegetation might be the effect of lower temperatures and/or of low atmospheric $CO_2$ during the glacial. Glacial temperatures being 5–6 K lower than today have been estimated by isotope studies on speleothems (Talma and Vogel, 1992; Holmgren et al., 2003). However, in case of the effects of low $CO_2$ also grasses should have increased, which is not found in our pollen record. Albeit a minor increase in Poaceae pollen percentages is found for MIS 8, 6, and 2 to 4, values remain under 20 % indicating no substantial increase of open savannah – let alone $C_4$ grass dominance – occurred in the region of the lower Limpopo River or in the Lebombos Hills. Other studies report limited increase of $C_4$ grasses in South Africa related to colder

and drier periods alternating with more humid ones during MIS 4-2 (Holzkämper et al., 2009; Bar-Matthews et al., 2009; Chase, 2010).

Comparing the abundances of EM2 – open mountainous scrubland with Fynbos affinities – with the stacked SST curve from our site (Caley et al., 2011) the correlation between the two is striking (Fig. 5). We performed a cross correlation between both curves showing coherency between SST and EM2 abundances at confidence levels exceeding 95 % for all periodicities longer than 25 ka. SST and EM2 abundances are perfectly in anti-phase (Table 2) suggesting that vegetation change in southeast Africa is directly anti-correlated with the SST of the Agulhas Current. At present, the influence of the Agulhas Current is mainly through the increase of South African summer rainfall with increasing SST and vice versa (Jury et al., 1993; Reason and Mulenga, 1999). Our data indicate that this relation has been valid for at least the past 350 ka covering several glacial-interglacial cycles.

The plants contributing to the EM2-signal are not specifically adapted to aridity but partly (e.g. Ericaceae) to a combination of cold/cool and dry conditions. The spread of mountainous vegetation indicates lower air temperatures during the glacial, while the correlation with lower SST accentuates the relation between lower precipitation and glacial vegetation. The paradox may lie in a moderate change of the net freshwater flux (precipitation minus evaporation). Air temperature over South Africa is calculated by different coupled ocean-atmosphere models to have been lower by ∼3 to 4 K during the Last Glacial Maximum (Bush and Philander, 1999; Shin et al., 2003). SST of the south-western Indian Ocean is modelled to have been 2 to 3 K lower (opt. cit.), while our SST-stack indicates maximally 3 K lower SSTs during glacial periods (Caley et al., 2011). According to Bush and Philander (1999) the net freshwater flux between the Last Glacial Maximum and the present day changed little, because the reduced rainfall is offset by reduced air temperature. Cooler temperatures combined with moderate drought during glacials might have been the driver of the considerable extension of mountain vegetation in eastern South Africa.

## 6.5   Other influences on eastern South African vegetation and climate

Apart from the dominating glacial-interglacial variability higher frequency rhythms are found in the vegetation record. To explore the possible orbital forcing of the vegetation we executed cross spectral analysis on the Endmember abundances comparing them to the normalised and stacked eccentricity, obliquity, and negative precession (ETP). EM1 shows power coherent with ETP at the precession (although only at 18.3 ka) and eccentricity bands, and EM2 shows coherency in the obliquity and eccentricity bands. We give phase lags if coherency is non-zero (Table 2). As the three endmembers sum up to 1, the spectrum of EM3 is dependent on the other two and a separate interpretation of it not meaningful.

Comparing EM1 abundances to the local summer insolation (December, 30° S) suggests a positive response of the humid mountain forest to increased insolation (Fig. 4). The power spectrum of EM1 shows several significant maxima (between 143–103 ka, at 49, 25, and 19 ka) of which the latter is coherent with insolation (Table 2, Fig. 7). The phase lag of 40° with the insolation maximum amounts to ca. 2 ka. The wavelet analysis indicates that power in the precession band occurs mainly between 120–135 ka and 190–220 ka (Fig. 8), when precession variability in the insolation is large. It seems that the higher frequency variability in EM1 (humid mountain forest) is associated with local summer insolation, which is also in phase with Northern Hemisphere winter insolation as predicted by the model of Laepple and Lohmann (2009). Their study uses the regional seasonal variation to model glacial interglacial temperature variability. The local response in a winter sensitive area at the Southern Hemisphere such as the southern African summer rain area south of ~20° S correlates to Northern Hemisphere insolation using Southern Hemisphere forcing (Laepple and Lohmann, 2009).

We distinguish here between the African summer rain area and the southern African monsoon area north of 20° S, which is summer sensitive meaning that the strongest effect on temperature change is in summer resulting in an anti-correlation with Northern Hemisphere summer insolation (Laepple and Lohmann, 2009). Through the

Title Page

Abstract | Introduction

Conclusions | References

Tables | Figures

◄◄ | ►►

◄ | ►

Back | Close

Full Screen / Esc

Printer-friendly Version

Interactive Discussion

subtropical anticyclones the monsoon may influence the summer rain region. According to Tyson and Preston-Whyte (2000) depends the influence of the Indian monsoon on how much subsidence from the upper-level outflow in July enhances the subtropical anticyclones affecting the subcontinent's aridity in winter. Indian monsoon air is
₅ also involved in the Intertropical Convergence Zone (Tyson and Preston-Whyte, 2000). However, as the Intertropical Convergence Zone over the African continent migrates between ca. 15° S and 20°N (Leroux, 1983) and while our study area is south of 24° S, the latter effect is probably not of major importance.

EM2 abundances show significant power at 100 and 40 ka that are explained by the
₁₀ tight fit of mountainous scrubland extension to SST variations in the western Indian Ocean (see previous section).


## 7 Conclusions

Pollen and spores have been retrieved from the upper half of core MD96-2048 covering the past 342 ka. Although the pollen concentration is low due to the relative low
₁₅ terrestrial input to the marine site, the vegetation development in the region north and west of Maputo could be studied for three complete climate cycles.

The pollen record shows strong glacial-interglacial variability alternating three different complexes of vegetation formations; (i) woodland and forest in the lowlands with grasslands on the interior plateau during full interglacial periods, (ii) open mountain-
₂₀ ous scrubland with Fynbos affinities during most of each glacial, and (iii) mountainous *Podocarpus* forest and woodlands during cool and humid intermediate periods.

Comparison with SST estimates from the same core showed that the extension of the mountainous scrubland is tightly coupled to the Agulhas Current system. This is explained by the strong influence sea surface temperatures of the western Indian Ocean
₂₅ have on the summer precipitation of northern South Africa and southern Mozambique.

The variation of the mountainous forest record along with precession is associated with the effects of Southern Hemisphere summer insolation on regional temperatures.

# References

Bar-Matthews, M., Marean, C. W., Jacobs, Z., Karkanas, P., Fischer, E. C., Herries, A. I. R., Brown, K., Williams, H. M., Bernatchez, J., Ayalon, A., and Nilssen, P. J.: A high resolution and continuous isotopic speleothem record of paleoclimate and paleoenvironment from 90 to

10  53 ka from Pinnacle Point on the south coast of South Africa, Quaternary Sci. Rev., 29, 2131–2145, 2010.

Beuning, K. R. M., Zimmerman, K. A., Ivory, S. J., and Cohen, A. S.: Vegetation response to glacial–interglacial climate variability near Lake Malawi in the southern African tropics, Palaeogeogr. Palaeocl., 303, 81–92, 2011.

15  Bonnefille, R. and Riollet, G.: The Kashiru pollen sequence (Burundi). Palaeoclimatic implications for the last 40,000 yr. B.P. in tropical Africa, Quaternary Res., 30, 19–35, 1988.

Botha, G. A., Scott, L., Vogel, J. C., and Von Brunn, V.: Palaeosols and palaeoenvironments during the Late Pleistocene Hypothermal in northern Natal, S. Afr. J. Sci., 88, 508-512, 1992.

Bush, A. B. G. and Philander, S. G. H.: The climate of the Last Glacial Maximum: Results

20  from a coupled atmosphere-ocean general circulation model, J. Geophys. Res., 104(D20), 24509–24525, 1999.

Caley, T., Kim, J.-H., Malaizé, B., Giraudeau, J., Laepple, T., Caillon, N., Charlier, K., Rebaubier, H., Rossignol, L., Castañeda, I. S., Schouten, S., and Damsté, J. S. S.: High-latitude obliquity forcing drives the agulhas leakage, Clim. Past Discuss., 7, 2193–2215, doi:10.5194/cpd-7-

25  2193-2011, 2011.

Chase, B.: South African palaeoenvironments during marine oxygen isotope stage 4: a context for the Howiesons Poort and Still Bay industries, J. Archaeol. Sci., 37, 1359–1366, 2010.

Chase, B. M. and Meadows, M. E.: Late Quaternary dynamics of southern Africa's winter rainfall zone, Earth-Sci. Rev., 84, 103–138, 2007.

**CPD**

7, 2261–2296, 2011

**Glacial-interglacial vegetation dynamics in south eastern Africa**

L. M. Dupont et al.

Title Page

| Abstract | Introduction |
| Conclusions | References |
| Tables | Figures |

|◀ | ▶|

◀ | ▶

Back | Close

Full Screen / Esc

Printer-friendly Version

Interactive Discussion

Coates Palgrave, K.: Trees of Southern Africa, 3rd edition, revised and updated, Struik, Cape Town, 2002.

Coetzee, J. A.: Pollen analytical studies in east and southern Africa, Palaeoeco. Afr., 3, 1–146, 1967.

Cohen, A. S., Stone, J. R., Beuning, K. R. M., Park, L. E., Reinthal, P. N., Dettman, D., Scholz, C. A., Johnson, T. C., King, J. W., Talbot, M. R., Brown, E. T., and Ivory, S. J.: Ecological consequences of early Late Pleistocene megadroughts in tropical Africa, P. Natl. Acad. Sci., 104, 16422–16427, 2007.

Debusk, G.H.: A 37,500-year pollen record from Lake Malawi and implications for the biogeography of afromontane forests, J. Biogeogr., 25, 479–500, 1998.

Elenga, H., Peyron, O., Bonnefille, R., Jolly, D., Cheddadi, R., Guiot, J., Andrieu, V., Bottema, S., Buchet, G., De Beaulieu, J.-L., Hamilton, A. C., Maley, J., Marchant, R., Perez-Obiol, R., Reille, M., Riollet, G., Scott, L., Straka, H., Taylor, D., Van Campo, E., Vincens, A., Laarif, F., and Jonson, H.: Pollen-based biome reconstruction for southern Europe and Africa 18,000 yr BP, J. Biogeogr., 27, 621–634, 2000.

Gasse, F. and Van Campo, E.: A 40,000-yr pollen and diatom record from Lake Tritrivakely, Madagascar, in the southern tropics, Quaternary Res., 49, 299–311, 1998.

Gasse, F. and Van Campo, E.: Late Quaternary environmental changes from a pollen and diatom record in the southern tropics (Lake Tritrivakely, Madagascar), Palaeogeogr. Palaeocl., 167, 287–308, 2001.

Gasse, F., Chalié, F., Vincens, A., Williams, M. A. J., and Williamson, D.: Climatic patterns in equatorial and southern Africa from 30,000 to 10,000 years ago reconstructed from terrestrial and near-shore proxy data, Quaternary Sci. Rev., 27, 2316–2340, 2008.

Heine, K.: The main stages of the late Quaternary evolution of the Kalahari region, southern Africa, Palaeoeco. A., 15, 53–76, 1982.

Henn, B. M., Gignoux, C. R., Jobin, M., Granka, J. M., Macpherson, J. M., Kidd, J. M., Rodríguez-Botigué, L., Ramachandran, S., Hon, L., Brisbin, A., Lin, A. A., Underhill, P. A., Comas, D., Kidd, K. K., Norman, P. J., Parham, P., Bustamante, C. D., Mountain, J. L., and Feldman, M. W.: Hunter-gatherer genomic diversity suggests a southern African origin for modern humans, P. Natl. Acad. Sci., 108, 5154–5162, 2011.

Henshillwood, C. S., d'Errico, F., Marean, C. W., Milo, R. G., and Yates, R.: An early bone tool industry from the Middle Stone Age at Blombos Cave, South Africa: implications for the origins of modern human behaviour, symbolism and language, J. Hum. Evol., 41, 631–678,

2001.

Henshillwood, C. S., d'Errico, F., and Watts, I.: Engraved ochres from the Middle Stone Age levels at Blombos Cave, South Africa, J. Hum. Evol., 57, 27–47, 2009.

Holmgren, K., Lee-Thorp, J. A., Cooper, G. R. J., Lundblad, K., Partridge, T. C., Scott, L., Sithaldeen, R., Talma, A. S., and Tyson, P. D.: Persistent millennial-scale climatic variability over the past 25,000 years in Southern Africa, Quaternary Sci. Rev., 22, 2311–2326, 2003.

Holzkämper, S., Holmgren, K., Lee-Thorp, J., Talma, S., Mangini, A., and Partridge, T.: Late Pleistocene stalagmite growth in Wolkberg Cave, South Africa, Earth Planet. Sc. Lett., 282, 212–221, 2009.

Jacobs, Z., Roberts, R. G., Galbraith, R. F., Deacon, H. J., Grün, R., Mackay, A., Mitchell, P., Vogelsang, R., and Wadley, L.: Age for the Middle Stone Age of Southern Africa: Implications for human behaviour and dispersal, Science, 322, 733–735, 2008.

Jury, M. R., Valentine, H. R., and Lutjeharms, J. R.: Influence of the Agulhas Current on summer rainfall along the southeast coast of South Africa, J. Appl. Meteorol., 32, 1282-1287, 1993.

Kersberg, H.: Afrika-Kartenwerk Serie S: Südafrika (Moçambique, Swaziland, Republik Südafrika), Bl. 7, Vegetationsgeographie, Gebrüder Bornträger, Berlin, 1985.

Kersberg, H.: Beiheft zu Afrika-Kartenwerk Serie S: Südafrika (Moçambique, Swaziland, Re-publik Südafrika), Bl. 7, Vegetationsgeographie, Gebrüder Bornträger, Berlin, 1996.

Kirsten, I., Fuhrmann, A., Thorpe, J., Roehl, U., and Oberhaensli, H.: Hydrological changes in Southern Africa over the last 200 Ka as recorded in lake sediments from Tswaing impact crater, S. Afr. J. Geol., 110, 311–326, 2007.

Laepple, T. and Lohmann, G.: Seasonal cycle as template for climate variability on astronomical timescales, Paleoceanography, 24, PA4201, doi:10.1029/2008PA001674, 2009.

Laskar, J., Robutel, P., Joutel, F., Gastineau, M., Correia, A. C. M., and Levrard, B.: A long-term numerical solution for the insolation quantities of the Earth, Astron. Astrophys., 428, 261–285, 2004.

Lee-Thorp, J. A. and Beaumont, P. B.: Vegetation and seasonality shifts during the Late Quaternary deduced from $^{13}$C/$^{12}$C ratios of grazers at Equus Cave, South Africa, Quaternary Res., 43, 426–432, 1995.

Leroux, M.: Le climat de L'Afrique tropicale, texte and atlas, Champion, Paris, 1983.

Lisiecki, L. E. and Raymo. M. E.: A Pliocene-Pleistocene stack of 57 globally distributed benthic $\delta^{18}$O records, Paleoceanography, 20, PA1003, doi:10.1029/2004PA001071, 2005.

Title Page

Abstract | Introduction

Conclusions | References

Tables | Figures

◄ | ►

◄ | ►

Back | Close

Full Screen / Esc

Printer-friendly Version

Interactive Discussion

Lutjeharms, J. R. E. and Da Silva, A. J.: The Delagoa Bight eddy, Deep-Sea Res., 35, 619–634, 1988.

Marean, C. W., Bar-Matthews, M., Bernatchez, J., Fischer, E., Goldberg, P., Herries, A. I. R., Jacobs, Z., Jerardino, A., Karkanas, P., Minichillo, T., Nilssen, P. J., Thompson, E., Watts, I., and Williams, H. M.: Early human use of marine resources and pigment in South Africa during the Middle Pleistocene, Nature, 449, 905–908, 2007.

Martin, A. K.: The influence of the Agulhas Current on the physiographic deveopment of the northernmost Natal Valley (S. W. Indian Ocean), Mar. Geol., 39, 259–276, 1981.

Paillard, D., Labeyrie, L., and Yiou, P.: Macintosh program performs time-series analysis, EOS Transact. AGU, 77, 379, 1996.

Partridge, T. C., DeMenocal, P. B., Lorentz, S. A., Paiker, M. J., and Vogel, J. C.: Orbital forcing of climate over South Africa: a 200,000-year rainfall record from the Pretoria Saltpan, Quaternary Sci. Rev., 16, 1125–1133, 1997.

Partridge, T. C., Scott, L., and Hamilton, J. E.: Synthetic reconstructions of southern African environments during the Last Glacial Maximum (21–18 kyr) and the Holocene Altithermal (8–6 kyr), Quatern. Int., 57–58, 207–214, 1999.

Reason, C. J. C. and Mulenga, H.: Relationships between South African rainfall and SST anomalies in the Southwest Indian Ocean, Int. J. Climatol., 19, 1651–1673, 1999.

Scott, L.: A late Quaternary pollen record from the Transvaal bushveld, South Africa, Quaternary Res., 17, 339–370, 1982a.

Scott, L.: Late Quaternary fossil pollen grains from the Transvaal, South Africa, Rev. Palaeobot. Palyno., 36, 241–278, 1982b.

Scott, L.: Pollen analysis of Hyena coprolites and sediments from Equus Cave, Tauung, Southern Kalahari (South Africa), Quaternary Res., 28, 144–156, 1987.

Scott, L.: Climatic conditions in Southern Africa since the last glacial maximum, inferred from pollen analysis, Palaeogeogr. Palaeocl., 70, 345–353, 1989.

Scott, L.: Vegetation history and climate in the Savanna biome South Africa since 190,000 ka: a comparison of pollen data from the Tswaing Crater (the Pretoria Saltpan) and Wonderkrater, Quatern. Int., 57–58, 215–223, 1999.

Scott, L. and Thackeray, J. F.: Multivariate analysis of late Pleistocene and Holocene pollen spectra from Wonderkrater, Transvaal, South Africa, S. Afr. J. Sci., 83, 93–98, 1987.

Glacial-interglacial vegetation dynamics in south eastern Africa

L. M. Dupont et al.

Title Page

| Abstract | Introduction |
| Conclusions | References |
| Tables | Figures |

Back | Close

Full Screen / Esc

Printer-friendly Version

Interactive Discussion

Scott, L. and Woodbone, S.: Pollen analysis and dating of Late Quaternary faecal deposits (hyraceum) in the Cederberg, Western Cape, South Africa, Rev. Palaeobot. Palyno., 144, 123–134, 2007.

Scott, L., Holmgren, K., Talma, A. S., Woodborne, S., and Vogel, J. C.: Age interpretation of the Wonderkrater spring sedmients and vegetation change in the Savanna Biome, Limpopo province, South Africa, S. Afr. J. Sci., 99, 484–488, 2003.

Shi, N., Schneider, R., Beug, H.-J., and Dupont, L. M.: Southeast trade wind variations during the last 135 kyr: evidence from pollen spectra in eastern South Atlantic, Earth Planet. Sc. Lett., 187, 311–321, 2001.

Shin, S.-I., Liu, Z., Otto-Bliesner, B., Brady, E. C., Kutzbach, J. E., and Harrison, S. P.: A simulation of the Last Glacial Maximum climate using the NCAR-CCSM, Clim. Dynam., 20, 127–151, 2003.

Stuut, J.-B., Crosta, X., van der Borg, K., and Schneider, R.: Relationship between Antartic sea ice and southwest African climate during the late Quaternary, Geology, 32, 909–912, 2004.

Talma, A. S. and Vogel, J. C.: Late Quaternary paleotemperatures derived from a speleothem from Cango Caves, Cape Province, South Africa, Quaternary Res., 37, 203–213, 1992.

Torrence, C. and Compo, G. P.: A Practical Guide to Wavelet Analysis, B. Am. Meteorol. Soc., 79, 61–78, 1998.

Tyson, P. D. and Preston-Whyte, R. A.: The weather and climate of Southern Africa, Oxford University Press, Cape Town, 2000.

Van Campo, E., Duplessy, J. C., Prell, W. L., Barratt, N., and Sabatier, R.: Comparison of terrestrial and marine temperature estimates for the apst 135 kyr off southeast Africa: a test for GCM simulations of palaeoclimate, Nature, 348, 209–212 1990.

Vincens, A., Garcin, Y., and Buchet, G.: Influence of rainfall seasonality on African lowland vegetation during the Late Quaternary: pollen evidence from Lake Masoko, Tanzania, J. Biogeogr., 34, 1274–1288, 2007.

Wadley, L.: Announcing a Still Bay industry at Sibudu Cave, South Africa, J. Hum. Evol., 52, 681–689, 2007.

Weltje, G. J.: End-member modeling of compositional data: numerical-statistical algorithms for solving the explicit mixing problem, Math. Geol., 29, 503–549, 1997.

White, F.: The vegetation of Africa, Natural Rescourses Research, UNESCO, Paris, 20, 1983.

Title Page

Abstract | Introduction

Conclusions | References

Tables | Figures

|◀ | ▶|

◀ | ▶

Back | Close

Full Screen / Esc

Printer-friendly Version

Interactive Discussion

**Table 1.** List of grouped pollen taxa occurring in 5 or more samples. Grouping was done using Kersberg (1996) and Coates Palgrave (2002). The columns EM1, EM2, EM3 denote the scores (in percent) of the taxa on each of the endmember assemblage EM1, EM2, or EM3, respectively (highest scores in bold). $r^2$ is the coefficient of determination (n.s., not significant). See methods for details of the endmember modelling unmixing procedure (Weltje, 1997).

| Pollen type | Family | EM1 | EM2 | EM3 | $r^2$ |
|---|---|---|---|---|---|
| Cyperaceae | | 18.98 | **42.37** | 28.26 | 0.39 |
| Poaceae | | 7.63 | 14.04 | **19.53** | 0.42 |
| *Podocarpus* | Podocarpaceae | **52.19** | 18.02 | 10.14 | 0.66 |
| Asteraceae | | | | | |
| Asteroideae pp | Asteraceae | 0.50 | 4.30 | **4.35** | 0.31 |
| Cichorioideae pp | Asteraceae | | n.s. | | |
| *Cotula*-type | Asteraceae | 0.00 | 0.10 | **0.68** | 0.29 |
| daisy-type | Asteraceae | 0.18 | **1.18** | 0.71 | 0.10 |
| *Gazania*-type | Asteraceae | | n.s. | | |
| *Pentzia*-type | Asteraceae | 0.00 | 0.77 | **1.30** | 0.18 |
| *Stoebe*-type | Asteraceae | 0.00 | **1.18** | 0.16 | 0.19 |
| *Tarchonanthus/Artemisia* | Asteraceae | | n.s. | | |
| *Vernonia* | Asteraceae | | n.s. | | |
| forest trees | | | | | |
| *Buxus madagascaria*-type | Buxaceae | | n.s. | | |
| Celastraceae | | 0.00 | 0.02 | **0.09** | 0.04 |
| *Chrysophyllum* | Sapotaceae | 0.00 | 0.07 | **0.25** | 0.16 |
| *Crotalaria* | Fabaceae | 0.11 | 0.00 | **0.16** | 0.05 |
| *Garcinia* | Clusiaceae | **0.26** | 0.00 | **0.26** | 0.06 |
| *Hymenocardia* | Euphorbiaceae | **0.33** | 0.00 | 0.20 | 0.10 |
| *Ilex* | Aquifoliaceae | | n.s. | | |
| *Khaya*-type | Meliaceae | 0.03 | 0.00 | **0.51** | 0.21 |

Title Page

Abstract | Introduction

Conclusions | References

Tables | Figures

Back | Close

Full Screen / Esc

Printer-friendly Version

Interactive Discussion

**Table 1.** Continued.

| | | | | | |
|---|---|---|---|---|---|
| *Lophira* | Ochnaceae | | | n.s. | |
| *Macaranga* | Euphorbiaceae | | | n.s. | |
| *Mallotus*-type | Euphorbiaceae | 1.24 | 0.06 | **2.65** | 0.17 |
| Meliaceae/Sapotaceae | | | | n.s. | |
| Schizeaceae | | **0.45** | 0.38 | 0.00 | 0.04 |
| *Tetrorchidium*-type | Euphorbiaceae? | 0.00 | **0.16** | 0.14 | 0.08 |
| Thymelaeaceae pp | | | | n.s. | |
| *Zanthoxylum* | Rutaceae | | | n.s. | |
| woodland trees and scrubs | | | | | |
| *Acacia* | Mimosaceae | | | n.s. | |
| Acanthaceae pp | | 0.06 | 0.00 | **0.26** | 0.09 |
| *Alchornea* | Euphorbiaceae | 0.89 | 0.03 | **3.69** | 0.47 |
| *Balanites* | Balanitaceae | 0.08 | 0.08 | **0.73** | 0.18 |
| *Brachystegia* | Caesalpiniaceae | 0.01 | 0.11 | **0.73** | 0.13 |
| *Bridelia* | Euphorbiaceae | | | n.s. | |
| *Burkea africana* | Caesalpiniaceae | 0.46 | 0.00 | **0.66** | 0.18 |
| *Cassia*-type | Caesalpiniaceae | 0.43 | 0.00 | **1.04** | 0.08 |
| *Celtis* | Ulmaceae | **0.70** | 0.00 | 0.21 | 0.11 |
| *Cleome* | Capparaceae | 0.07 | 0.00 | **0.07** | 0.07 |
| *Coffea*-type | Rubiaceae | | | n.s. | |
| Combretaceae pp | | 0.20 | 0.14 | **1.14** | 0.23 |
| *Croton* | Euphorbiaceae | | | n.s. | |
| *Daniellia*-type | Fabaceae | 0.11 | 0.00 | **0.42** | 0.20 |
| *Diospyros* | Ebenaceae | | | n.s. | |
| *Dodonaea viscosa* | Sapindaceae | 0.27 | 0.09 | **0.77** | 0.11 |
| *Dombeya* | Sterculiaceae | | | n.s. | |
| *Dracaena* | Agavaceae | | | n.s. | |
| *Euclea* | Ebenaceae | | | n.s. | |
| *Euphorbia* | Euphorbiaceae | 0.58 | 0.00 | **1.32** | 0.19 |
| Fabaceae pp. | | 0.18 | 0.00 | **0.50** | 0.09 |

**Glacial-interglacial vegetation dynamics in south eastern Africa**

L. M. Dupont et al.

Title Page

Abstract | Introduction

Conclusions | References

Tables | Figures

◄ | ►

Back | Close

Full Screen / Esc

Printer-friendly Version

Interactive Discussion

**Table 1.** Continued.

| | | | | | |
|---|---|---|---|---|---|
| *Grewia* | Tiliaceae | | n.s. | | |
| *Hyphaene* | Arecaceae | 0.07 | **0.21** | 0.07 | 0.04 |
| *Hypoestes*-type | Acanthaceae | | n.s. | | |
| *Indigofera*-type | Fabaceae | 0.15 | 0.04 | **0.30** | 0.05 |
| *Klaineanthus* | Euphorbiaceae | | n.s. | | |
| *Lannea/Sclerocarya* | Anacardiaceae | 0.03 | 0.00 | **0.36** | 0.12 |
| *Manilkara*-type | Sapotaceae | 0.58 | 0.00 | **0.61** | 0.13 |
| *Parinari* | Chrysobalanaceae | 0.04 | 0.00 | **0.08** | 0.05 |
| *Peltophorum africanum* | Caesalpiniaceae | **0.15** | 0.00 | 0.07 | 0.06 |
| *Philenoptera*-type | Fabaceae | | n.s. | | |
| *Pterocarpus*-type | Fabaceae | | n.s. | | |
| Rhamnaceae pp | | | n.s. | | |
| *Rhus* | Anacardiaceae | | n.s. | | |
| Rubiaceae pp | | 0.04 | 0.00 | **0.13** | 0.05 |
| Sapotaceae pp | | | n.s. | | |
| *Schrebera*-type | Oleaceae | 0.27 | 0.00 | **0.65** | 0.14 |
| *Sorindeia juglanifolia*-type | Anacardiaceae | | n.s. | | |
| *Spermacoce* | Rubiaceae | 0.04 | 0.00 | 0.27 | 0.13 |
| *Tapinanthus* | Loranthaceae | | n.s. | | |
| *Tarchonanthus/Artemisia* | Asteraceae | | n.s. | | |
| *Tephrosia*-type | Fabaceae | | n.s. | | |
| *Uapaca* | Euphorbiaceae | 0.08 | **0.40** | 0.20 | 0.05 |
| *Urtica*-type | Urticaceae | **0.20** | 0.00 | 0.00 | 0.08 |

Mountainous herbs, scrubs and trees

| | | | | | |
|---|---|---|---|---|---|
| *Aloe*-type | Liliaceae | 0.05 | **0.34** | 0.17 | 0.04 |
| *Anthoceros* | Anthocerotaceae | | n.s. | | |
| *Anthospermum* | Rubiaceae | 0.27 | 0.29 | **0.88** | 0.07 |
| Ericaceae | | 0.19 | **6.23** | 1.85 | 0.47 |
| *Lycopodium* | Lycopodiaceae | | n.s. | | |
| *Lycopodium cernuum*-type | Lycopodiaceae | 0.04 | **0.14** | 0.00 | 0.05 |

Title Page

Abstract | Introduction

Conclusions | References

Tables | Figures

|◄ | ►|

◄ | ►

Back | Close

Full Screen / Esc

Printer-friendly Version

Interactive Discussion

Table 1. Continued.

| | | | | | |
|---|---|---|---|---|---|
| *Myrica* | Myricaceae | | | n.s. | |
| *Myrsine africana* | Myrsinaceae | **1.19** | 0.00 | 1.11 | 0.14 |
| *Olea* | Oleaceae | | | n.s. | |
| *Passerina* | Thymelaeaceae | 0.00 | **0.80** | 0.10 | 0.18 |
| *Phaeoceros* | Anthocerotaceae | 0.71 | **1.79** | 0.00 | 0.30 |
| *Protea/Faurea* | Proteaceae | 0.14 | 0.00 | **0.20** | 0.03 |
| *Pseudolachnostylis*-type | Euphorbiaceae | 0.14 | 0.00 | **0.58** | 0.19 |
| Restionaceae | | 0.15 | **0.52** | 0.00 | 0.05 |
| *Stoebe*-type | Asteraceae | 0.00 | **1.18** | 0.16 | 0.19 |

<table><tbody><tr><td colspan="6" align="center">Mangrove tree</td></tr></tbody></table>

| | | | | | |
|---|---|---|---|---|---|
| *Rhizophora* | Rhizophoraceae | 0.82 | 0.00 | **1.11** | 0.14 |

<table><tbody><tr><td colspan="6" align="center">Coastal and halophytic scrubs and herbs</td></tr></tbody></table>

| | | | | | |
|---|---|---|---|---|---|
| Aizoaceae | | 0.80 | 0.00 | **0.82** | 0.06 |
| *Boscia/Maerua* | Capparaceae | | | n.s. | |
| Caryophyllaceae | | | | n.s. | |
| Chenopodiaceae/Amaranthaceae | | 0.12 | 0.74 | **2.17** | 0.47 |
| *Gazania*-type | Asteraceae | | | n.s. | |
| *Polycarpaea* | Caryophyllaceae | **0.10** | 0.00 | 0.06 | 0.05 |
| *Raphia*-type | Arecaceae | | | n.s. | |
| *Tribulus* | Zygophyllaceae | 0.03 | 0.19 | **0.27** | 0.04 |
| *Ziziphus*-type | Rhamnaceae | | | n.s. | |

<table><tbody><tr><td colspan="6" align="center">Riparian and swamp plants</td></tr></tbody></table>

| | | | | | |
|---|---|---|---|---|---|
| Alismataceae pp | | **1.94** | 0.00 | 0.93 | 0.11 |
| *Borassus* | Arecaceae | | | n.s. | |
| Campanulaceae | | | | n.s. | |
| *Phoenix* | Arecaceae | | | n.s. | |
| *Polygonum senegalensis*-type | Polygonaceae | | | n.s. | |

Title Page

Abstract | Introduction

Conclusions | References

Tables | Figures

◄ | ►|

◄ | ►

Back | Close

Full Screen / Esc

Printer-friendly Version

Interactive Discussion

**Glacial-interglacial vegetation dynamics in south eastern Africa**
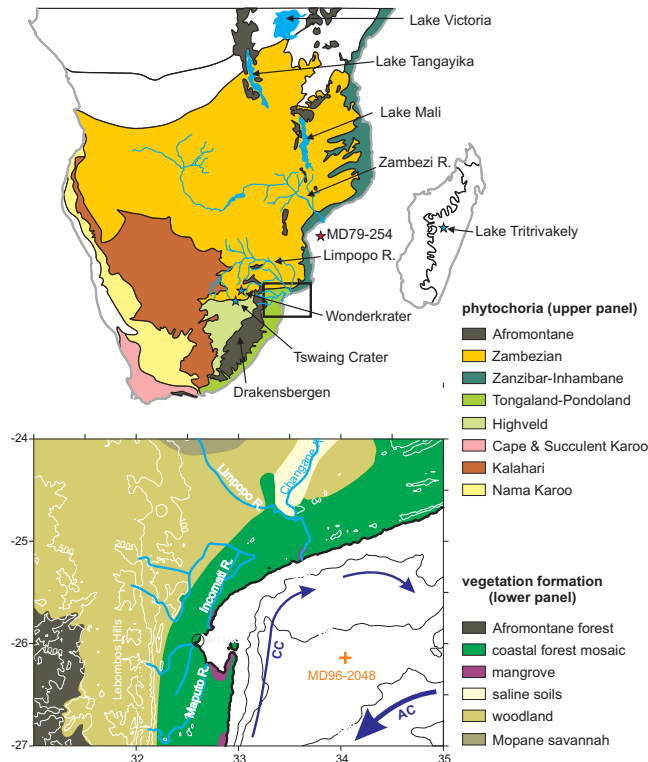
L. M. Dupont et al.

**Table 1.** Continued.

| | | | | | |
|---|---|---|---|---|---|
| *Pteris* | Pteridaceae | **0.48** | 0.13 | **0.49** | 0.04 |
| *Stipularia africana* | Rubiaceae | 0.00 | **0.11** | 0.04 | 0.04 |
| *Typha* | Thyphaceae | 0.26 | **0.83** | 0.27 | 0.05 |
| Not classified | | | | | |
| *Cnestis*-type | Conneraceae | | n.s. | | |
| *Evolvulus*-type | Convolvulaceae | | n.s. | | |
| *Plantago* | Plantaginaceae | | n.s. | | |
| *Solanum* | Solanaceae | | n.s. | | |
| stephanocolporate, striatoreticulate | Solanaceae? | | n.s. | | |

L. M. Dupont et al.

**Table 2.** Coherency (Coh.) and phase in degrees ($\varphi$) at orbital periodicities between end-members and ETP (normalised and stacked eccentricity, obliquity, and negative precession), between EM1 and mean December insolation at 30° S (Ins.), and between EM2 and SST (Caley et al., 2011). At a confidence level of 95 % coherence is non-zero if larger than 0.554. Phase is given in degrees in case of non-zero coherency.

| | 18.3 ka | | 23 ka | | 41 ka | | 100 ka | |
|---|---|---|---|---|---|---|---|---|
| | Coh. | $\varphi$ [°] | Coh. | $\varphi$ [°] | Coh. | $\varphi$ [°] | Coh. | $\varphi$ [°] |
| EM1 vs. ETP | 0.78 | $140 \pm 11$ | 0.54 | | 0.39 | | 0.64 | $32 \pm 16$ |
| EM2 vs. ETP | 0.39 | | 0.51 | | 0.76 | $138 \pm 11$ | 0.82 | $205 \pm 10$ |
| EM1 vs. Ins. | 0.80 | $317 \pm 10$ | 0.54 | | 0.32 | | 0.15 | |
| EM2 vs. SST | 0.53 | | 0.50 | | 0.89 | $183 \pm 7$ | 0.98 | $173 \pm 3$ |

**Fig. 1.** Upper panel: map of southern Africa with the main phytochoria after White (1983). Location of sites mentioned in the text are denoted by asterix. Lower panel: site location of MD96-2048; main vegetation formations; main rivers; 100 m, 200 m, 500 m, and 1000 m contours; 200 m, 500 m, and 1000 m bathymetric contours; Agulhas (AC) and counter currents (CC) forming a coastal eddy. Zambezian vegetation woodland and savannah north of ∼25°30′ S, Tongaland-Pondoland coastal forests south of ∼25°30′ S, Zanzibar-Inhambane coastal forests east of 33–34° E. West of the escarpment with Afromontane forest rises the interior plateau covered with Highveld grasslands.

Title Page

Abstract | Introduction

Conclusions | References

Tables | Figures

◀ | ▶

◀ | ▶

Back | Close

Full Screen / Esc

Printer-friendly Version

Interactive Discussion
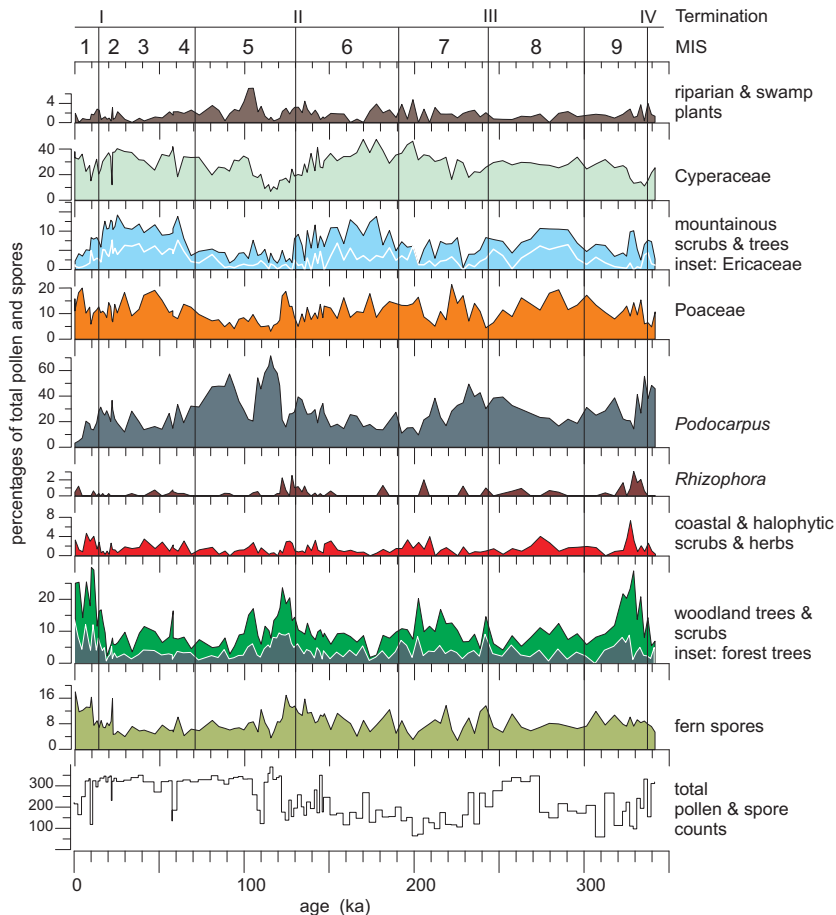
**Fig. 2.** Pollen percentages of groups (defined in Table 1) and selected taxa on the timescale of LR04 (Lisiecki and Raymo, 2004). Bottom curve shows the total of counted pollen and spores used in the percentage calculation. MIS, Marine Isotope Stage.

Title Page

Abstract | Introduction

Conclusions | References

Tables | Figures

◄ | ►

◄ | ►

Back | Close

Full Screen / Esc

Printer-friendly Version

Interactive Discussion
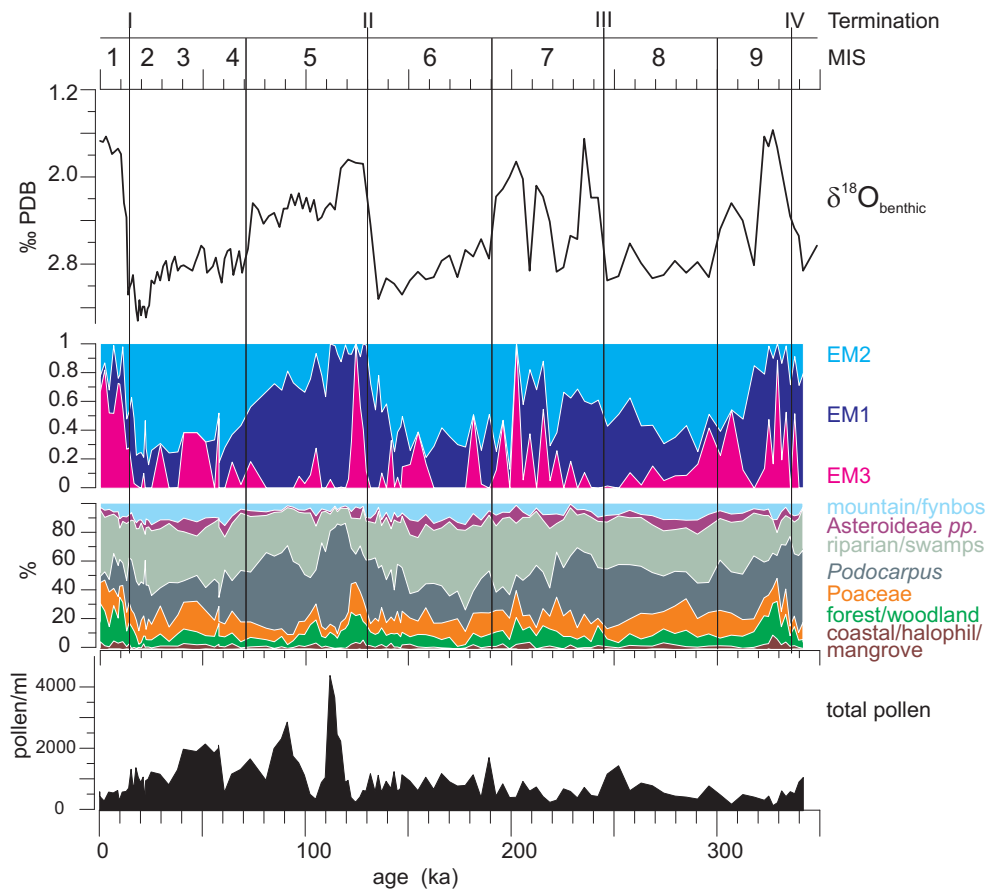
**Fig. 3.** Stable oxygen isotopes of benthic foraminifers per mille Pee Dee Belemnite (‰ PDB), cumulative Endmember abundances, summary pollen diagram (%), pollen concentration (ml). MIS, Marine Isotope Stage.

Title Page

Abstract | Introduction

Conclusions | References

Tables | Figures

|◄ | ►|

◄ | ►

Back | Close

Full Screen / Esc

Printer-friendly Version

Interactive Discussion
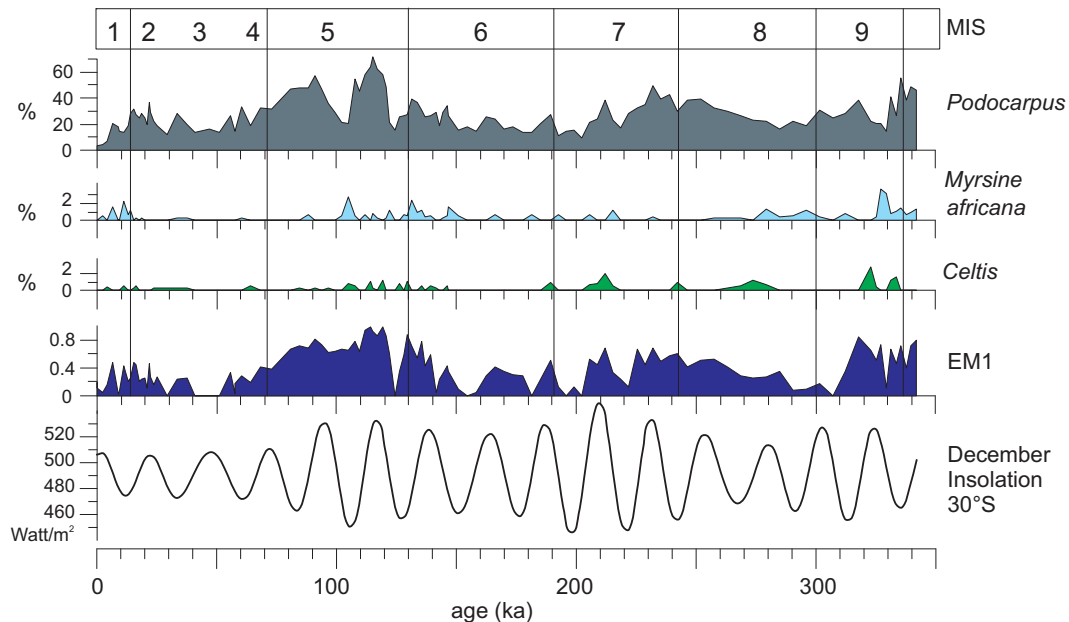
**Fig. 4.** Pollen percentages of selected taxa scoring relatively high on Endmember 1 (EM1). Bottom curve the mean December insolation at 30° S after Laskar et al. (2004). MIS, Marine Isotope Stage.
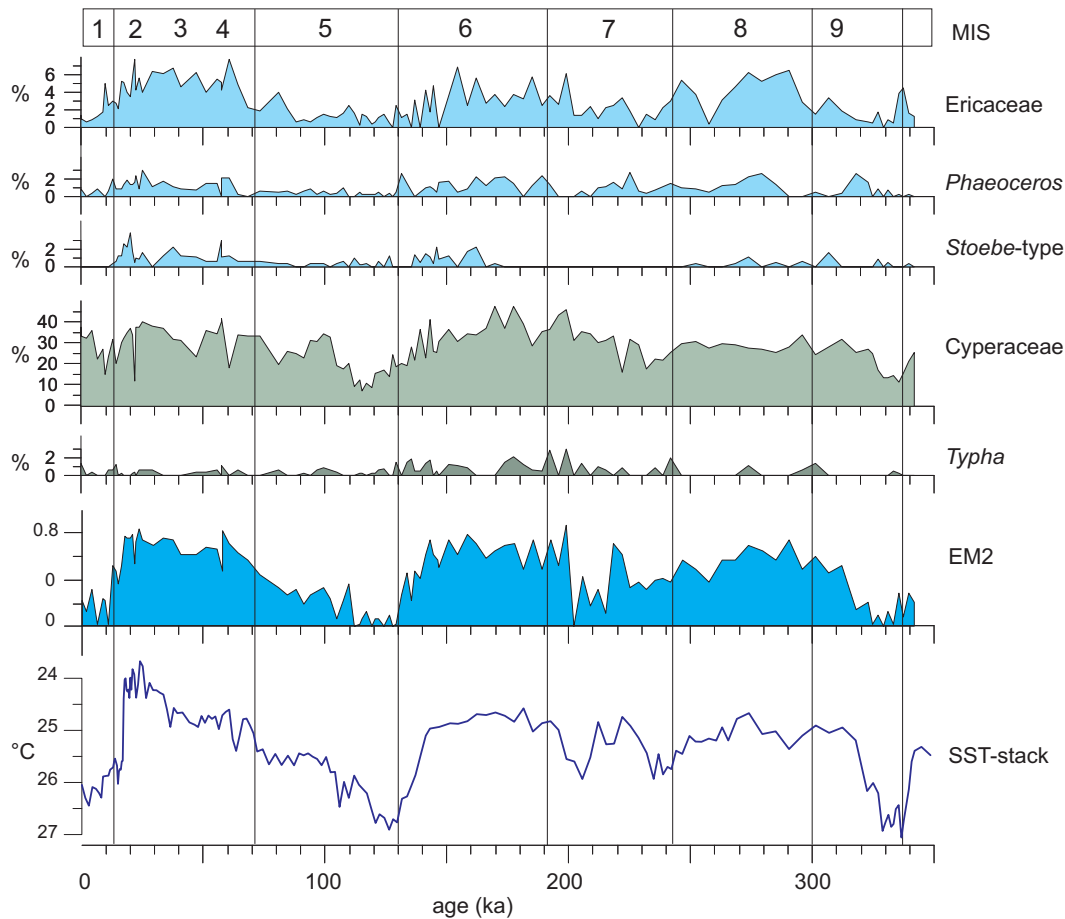
**Fig. 5.** Pollen percentages of selected taxa scoring relatively high on Endmember 2 (EM2), EM2 ratios, and SST-stack (Caley et al., 2011). Note the reversed y-axis of the SST-stack. MIS, Marine Isotope Stage.

Title Page

Abstract | Introduction

Conclusions | References

Tables | Figures

|◄ | ►|

◄ | ►

Back | Close

Full Screen / Esc

Printer-friendly Version

Interactive Discussion
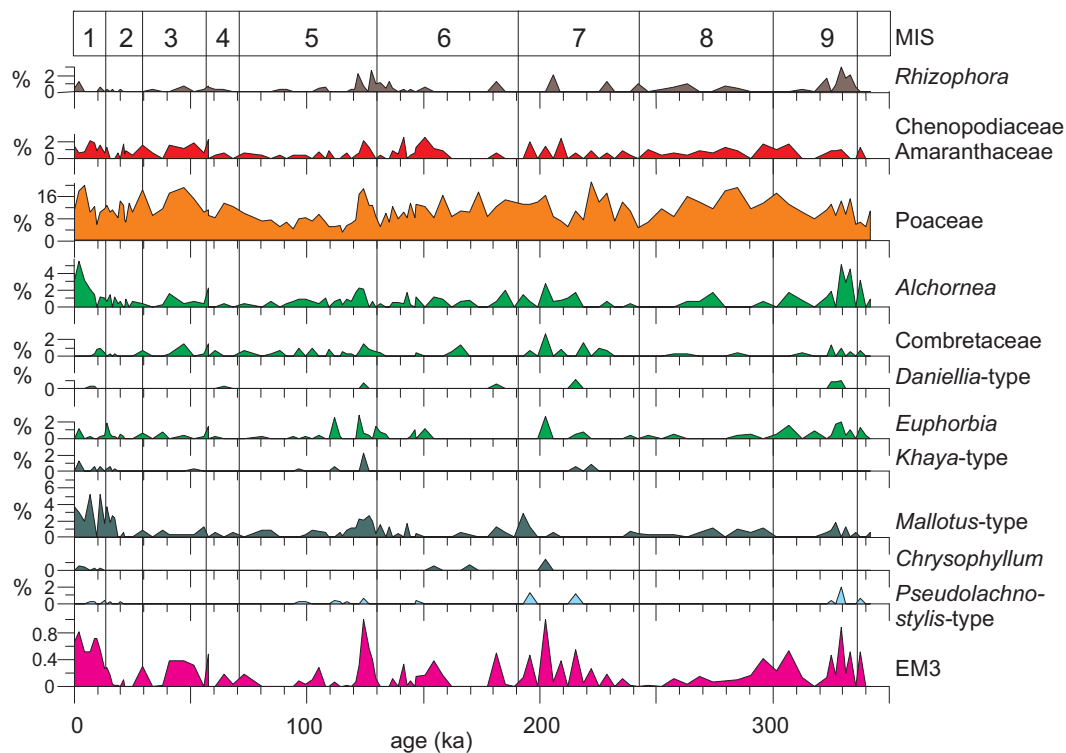
**Fig. 6.** Pollen percentages of selected taxa scoring relatively high on Endmember 3 (EM3). EM3 ratios at the bottom. MIS, Marine Isotope Stage.
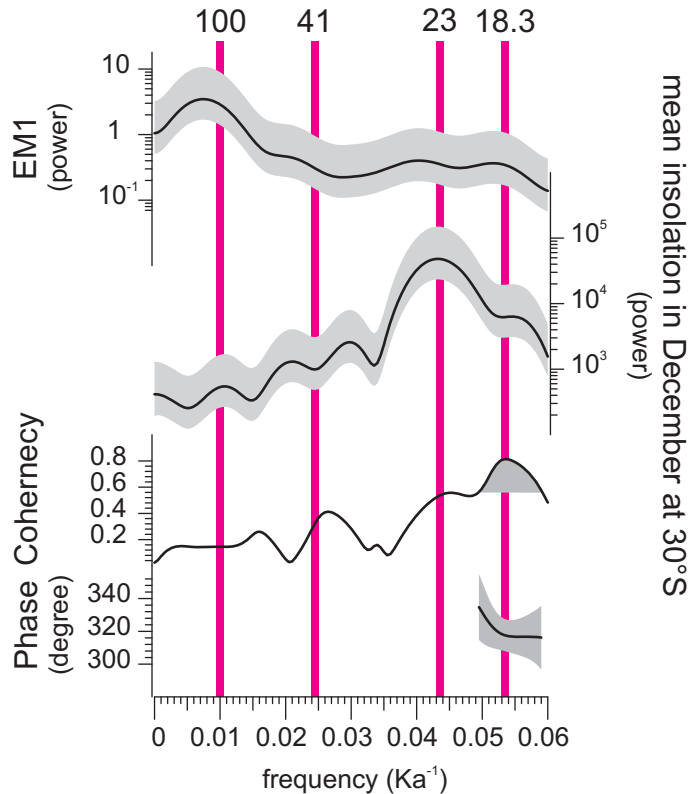
**Fig. 7.** Cross correlation between EM1 and mean December insolation at 30° S. From top to bottom: power spectra of EM1 (log scale left) and insolation (log scale right), coherency (non-zero coherency > 0.554, shaded), and phase in degrees. Confidence level is set at 95 %. Bandwidth is 0.014. Error ranges are shaded. Phase is only plotted if coherency is non-zero. Orbital periodicities in ka are denoted by pink bars. At the 18 ka precession band EM2 lags Southern Hemisphere December insolation by ∼40° (∼2 ka). Interpolations and calculations were carried out in AnalySeries (Paillard et al. 1996).

Title Page

Abstract | Introduction

Conclusions | References

Tables | Figures

◄◄ | ►►

◄ | ►

Back | Close

Full Screen / Esc

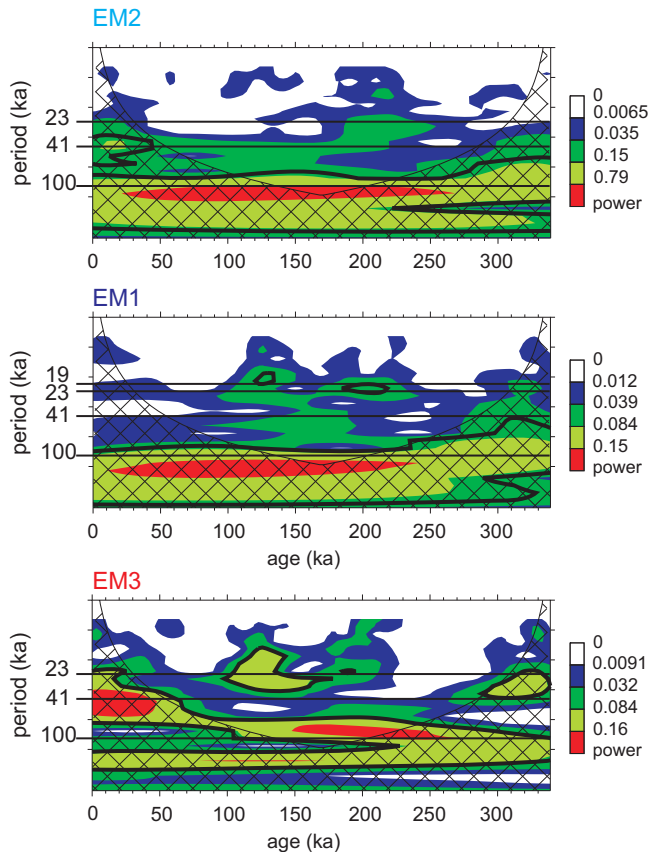Printer-friendly Version

Interactive Discussion

**Fig. 8.** Wavelet power spectra after Torrence and Compo (1998) for EM2 (top), EM1 (middle), EM3 (bottom). The contour levels are chosen so that 75 %, 50 %, 25 %, and 5 % of the wavelet power is above each level, respectively. The cross-hatched region is the cone of influence, where zero padding has reduced the variance. Black contour is the 90 % significance level, using a white-noise background spectrum.

Title Page

Abstract | Introduction

Conclusions | References

Tables | Figures

◄ | ►

Back | Close

Full Screen / Esc

Printer-friendly Version

Interactive Discussion